Biomass Electrochemistry : from cellulose to sorbitol

Kwon, Y.

8

Electrocatalytic hydrogenation of 5-hydroxymethylfurfural in the absence and presence of glucose

Abstract

This chapter addresses the electrocatalytic hydrogenation of 5-hydroxymethylfurfural (HMF) to 2,5-dihydroxymethylfuran (DHMF) or other species, such as 2,5-dimethylfuran, on solid metal electrodes in neutral media, both in the absence and presence of glucose. The reaction is studied by combining voltammetry with online product analysis by high-performance liquid chromatography, which provides both qualitative and quantitative information of the reaction products as a function of electrode potential. Three groups of catalysts show different selectivity towards: (1) DHMF (Fe, Ni, Ag, Zn, Cd, and In), (2) DHMF and other products (Pd, Al, Bi, and Pb), depending on the applied potential, and (3) other products (Co, Au, Cu, Sn, and Sb) involving HMF hydrogenolysis. The rate of electrocatalytic HMF hydrogenation is not strongly catalyst dependent since all catalysts show similar onset potentials (-0.5 ± 0.1 V) in the presence of HMF. However the intrinsic property of the catalysts determines the reaction pathway towards DHMF or other products. Ag showed highest activity towards DHMF formation (max. 13.1 mM cm^{-2} with high selectivity > 85%). HMF hydrogenation is faster than glucose hydrogenation on all metals. For transition metals, the presence of glucose enhances the formation of DHMF and suppresses the hydrogenolysis of HMF. On poor metals, glucose enhances the DHMF formation on Zn, Cd, and In, however, its contribution to Bi, Pb, Sn, and Sb is limited. Remarkably, in the presence of HMF, glucose hydrogenation itself is largely suppressed or even absent. The first electron transfer step of HMF reduction is not metal dependent suggesting a non-catalytic reaction with proton transfer directly from water in the electrolyte.

The contents of this chapter have been published: Y. Kwon, E. de Jong, S. Raoufmoghaddam, M. T. M. Koper, *ChemSusChem*, **2013**, DOI: 10.1002/cssc.201300443.

8.1 Introduction

Catalytic conversion of biomass to fuels and chemicals has attracted great attention as one of the future technologies for mitigating global warming and for building up a carbon-neutral energy cycle.[1, 2] 5-hydroxymethylfurfural (HMF), one of the novel biomass-derived platform chemicals, has potential as an alternative commodity chemical for fossil fuel-based platform chemicals.[3, 4] The chemistry, production processes and potential applications of HMF have recently been reviewed.[4] HMF has been produced from fructose in water, in organic solvents (DMSO),[5] and in a biphasic system (water-MIBK)[6] and in ionic liquids[7-10] using acid catalysts (i.e. HCl, H_2SO_4),[11] solid acids (zeolite,[6] ion exchange resins[12]), and salts ($LaCl_3$, $CrCl_2$)[13, 14]. Recently, HMF was obtained in high yields not only from fructose but also from glucose via isomerization to fructose, as well as directly from cellulose.[15-17]

HMF has two functionalities (-OH, -C=O) attached to a furan ring and it can be converted into several value-added compounds through oxidation and reduction. The oxidative products of HMF are 2,5-furandicarbaldehyde (FDC) and 2,5-furandicarboxylic acid (FDCA), which are excellent candidates for monomers of biomass derived polymeric materials.[18, 19] 2-formyl-5-furancarboxylic acid (FFCA) is also an intermediate species during HMF oxidation and it can be further oxidized to FDCA, a potential replacement for the fossil fuel-based platform chemical terephthalic acid.[20] For the oxidation of HMF, Strasser et al.[21] reported 100% conversion of HMF to DFCA with 80% selectivity using Pt/C at mild temperature (50^{o}C) and pressure (10 bar O_2), in comparison the with electrochemical oxidation of HMF to FDC (18%) on a Pt electrode. The hydrogenation of the formyl group or the furan ring on HMF to 2,5-dihydroxymethylfuran (DHMF) or di-hydroxy-methyl-tetrahydrofuran (DHMTHF) has been studied using heterogeneous catalysts based on Ni, Cu, Pt, Pd, and Ru[22] or bimetallic catalysts (i.e. Ni-Pd)[23]. DHMF is used in a broad field of applications such as resins, polymers, and artificial fibers, as well as an intermediate in the synthesis of drugs.[3] DHMTHF is a useful chemical with applications as solvent,[24] monomer,[18] or as a precursor to the production of other high-value chemicals.[25] The hydrogenation of the hydroxyl group on HMF leads to the formation of 2,5-dimethylfuran (DMF), which is of particular interest due to its high energy content and potential use as a biofuel.[26] DMF can be obtained on CuRu/C[26, 27] catalysts with high yield (76-79%). Although a large number of papers related to HMF

hydrogenation has been published, the hydrogenation of HMF using electrochemical methods has not yet been explored.

Recently, we studied the electocatalytic glucose hydrogenation in neutral media on a large number of pure solid metal electrodes from across the Periodic Table and successfully demonstrated the activity and selectivity of the various catalysts by correlating the voltammetry and product analysis with online high-performance liquid chromatography (HPLC).[28] Three groups of catalysts regarding reaction products could be distinguished: 1) hydrogen formation on early transition metals (Ti, V, Cr, Mn, Zr, Nb, Mo, Hf, Ta, We, and Re) and platinum group metals (Ru, Rh, Ir, and Pt), 2) sorbitol formation on late transition metals (Fe, Co, Ni, Cu, Pd, Au, and Ag) and Al (*sp* metal), and 3) sorbitol and 2-deoxysorbitol formation on post-transition metals (In, Sn, Sb, Pb, and Bi) as well as Zn and Cd (*d* metals). As HMF is a product of subsequent glucose dehydration during acid-catalysed cellulose hydrolysis,[29] there is a need to understand the effect of the presence of glucose on the hydrogenation of HMF and vice versa.

In this chapter, we investigated the electocatalytic HMF hydrogenation to DHMF and other products (i.e. 5-methylfurfural, 2,5-dimethylfuran, 2,5-dimethyl-2,3-dihydrofuran) in the absence and the presence of glucose on a large number of pure solid metal electrodes, which are all active for glucose hydrogenation, aiming at understanding the activity and selectivity of catalysts by correlating the voltammetry and online product analysis. Reaction products are determined both quantitatively and qualitatively by using a combination of voltammetry and online high-performance liquid chromatography (HPLC).[28-35] Finally, a general mechanism for electrocatalytic hydrogenation of HMF and the effect of the presence of glucose are discussed based on the observed activity and selectivity profiles during electrolysis.

8.2 Experimental

8.2.1 Electrochemical procedures

All measurements were carried out in a conventional single compartment three-electrode glass cell, which was cleaned by employing a standard procedure[36] for removing traces of

organic and inorganic contaminants. Oxygen was removed by bubbling argon through the solution prior to the voltammetric experiments. Transition and post-transition metals (≥99.5%) used as working electrodes in the experiment were polycrystalline wires/ rods/plates, which were mechanically polished with alumina (up to 0.05 μm) and cleaned ultrasonically in pure water (MilliQ gradient A10 system, 18.2 MΩ) followed by electropolishing by cycling 3 times between -2 and 0 V (vs. RHE) in 0.1 M Na_2SO_4 solution in order to remove surface impurities and oxide before use.[28] The surface area (cm^2) of the catalysts used to calculate the current density and concentration yield of reaction products (mM cm^{-2}) was obtained based on geometric area except for Pt electrode for which we considered the electrochemically active surface area by the hydrogen desorption charge in 0.5 M H_2SO_4. In all experiments, a large gold coil was used as a counter electrode while a reversible hydrogen electrode (RHE) was employed as a reference electrode. HMF (50 mM, Sigma-Aldrich), HMF (10 mM) and Glucose (0.1 M, Merck) were dissolved into a solution of 0.1 M Na_2SO_4 (Merck, pH 7). Electrochemical cell potentials were controlled with a potentiostat/galvanostat (μ-Autolab Type III). All experiments were carried out at room temperature.

8.2.2 Fraction collection and product analysis

For the detection of intermediates and products by HPLC, samples of the electrolyte solution were collected with a small Teflon tip (inner diameter, 0.38 mm) positioned close (10 μm) to the center of the electrode surface, the tip being connected to a PEEK capillary with inner/outer diameters of 0.13/1.59 mm.[30] The tip was cleaned in a solution of 0.2 M $K_2Cr_2O_7$ and rinsed thoroughly with ultrapure water before use. The sample volume collected in each well was 60 μl on a 96-well microtiter plate (270 μl/well, Screening Devices b.v.) using an automatic fraction collector (FRC-10A, Shimadzu). The flow rate of sample collection was adjusted to 60 ml min^{-1} with a Shimadzu pump (LC-20AT). Collected samples were immediately neutralized by adding 60 μl of 10 mM phosphate buffer. After collecting samples, the microtiter plate was covered by a silicon mat to prevent the evaporation of collected samples.

Samples collected during voltammetry were analysed using a Shimadzu Prominence HPLC. The microtiter plate with the collected samples was placed in an autosampler (SIL-20A) holder, and 30 μl of sample was injected into the column. The column (Shodex SP0810) for

the analysis used pure water as the eluent. The temperature of the column was maintained at 30°C for the mixture of HMF and glucose and at 50°C for HMF, respectively, in an oven (CTO-20A). The separated compounds were detected with a refractive index detector (RID-10A). The concentrations of DHMF and other products are obtained by using a Shodex SP0810 column and the detailed compositions of other products were confirmed by an Agilent Technologies 7820A + 5975 MSD GC-MS.

8.3 Results and discussion

In order to simplify the description of the product distribution, we use the term 'DHMF' for 2,5-dihydroxymethylfuran, which is the hydrogenation product of 'C=O' in HMF, and the term 'others' for the mixture of hydrogenolysis products (i.e. 5-methylfurfural, 2,5-dimethylfuran, 2,5-dimethyl-2,3-dihydrofuran) generated through the cleavage of the '-OH' functionality in HMF as shown in Scheme 1. The lump-sum of 'others' was obtained from the HPLC analysis whereas GC-MS identified each species. The details of hydrogenation pathways will be described later in Figure 6.

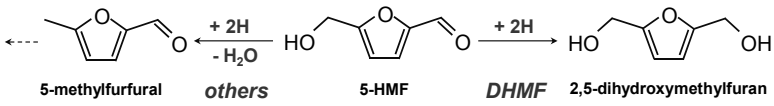

Scheme 1. HMF hydrogenation and dehydration pathways.

The metal catalysts studied are divided into three groups based on the dominant reaction products from HMF reduction in the absence of glucose; i) metals mainly forming DHMF (Fe, Ni, Ag, Zn, Cd, and In), ii) metals forming DHMF and others depending on the applied potential (Pd, Al, Bi, and Pb), and iii) metals forming mainly other products (Co, Au, Cu, Sn, and Sb). The same catalysts are compared for the reduction of a mixture of HMF and glucose. In the following sections, the term 'selectivity' is the percentage of the total of the reaction products from HMF i.e. DHMF, others, sorbitol or 2-deoxysorbitol, not taking into account hydrogen generation. The current density (mA cm^{-2}) and concentration yield of reaction products (mM cm^{-2}) to compare the catalytic activity were obtained based on geometric area of catalyst.

8.3.1 HMF reduction in the absence of glucose

Figure 1 shows the voltammograms of the HMF-free "blank" solution (dashed line) and of a solution containing 50 mM HMF (solid line) in 0.1 M Na_2SO_4 alongside the concentration profiles of the reaction products, DHMF and others, on (a) Fe, Ni, and Ag, (b) Pd and Al, and (c) Co, Au, and Cu. The cathodic current observed in the blank experiment (dashed line) is attributed to the evolution of H_2 and the solid line represents the formation of DHMF and other products from HMF reduction, as well as H_2 from hydrogen evolution reaction (HER). First of all, note that all transition metals in Figure 1 show different onset potentials for H_2 evolution in the blank scans within the potential ranges from -1 V to -0.4 V, which is consistent with our previous study.[28] For all metals, the onset potential in the presence of HMF in solution is the same or more positive compared to the blank. In the presence of HMF, the cathodic currents at high overpotentials are lower than those from blank scans, presumably due to HMF adsorption onto the electrode surface. Periodic spikes visible in the voltammograms with HMF on Cu and Ag are due to the irregularities in the pumping flow rate during fraction collection.[30] Although each metal shows a different catalytic activity, we observe certain trends in product distribution. According to the dominant reaction products, the transition metals are divided into three groups. The metals in Figure 1a show a higher activity towards DHMF formation than to other products over the entire potential range, whilst the metals in Figure 1c prefers to generate other products through hydrogenolysis of HMF over the production of DHMF. The metals in Figure 1b alternate their activity to DHMF and others depending on the applied potential.

Although Fe, Ni, and Ag show different onset potentials in the blank scans in Figure 1a, we note that in the presence of HMF, DHMF is generated from the same potential of ca. -0.4 V on each electrode. The maximum production of DHMF on these catalysts is observed at the potential of ca. -0.8 V. At higher potential H_2 evolution is dominant. On Fe, the other hydrogenolysis products are observed from -0.63 V and their concentrations increase as the cathodic potential increases. Therefore the selectivity of DHMF on Fe decreases from 100% at the onset potential to ca. 50% at -1.5 V. Ni shows the most positive onset potential in the blank and the highest current with HMF in solution. However the activity of Ni towards HMF hydrogenation is lower than that of Fe and Ag. The maximum concentration of DHMF on Ni is observed at -0.75 V whereas the other products on Ni are generated from -0.69 V and their concentrations increase gradually as the cathodic potential increases,

leading to a comparable selectivity towards DHMF and others at -1.5 V. Interestingly, the current density on Ag in the presence of HMF in solution is higher than that of blank from the onset potential until -1.3 V. The enhanced current is mainly due to the generation of DHMF since Ag shows the highest activity towards DHMF formation of all metal electrodes. The maximum concentration of DHMF on Ag is 13.1 mM cm^{-2} at -0.81 V. The selectivity of DHMF on Ag is higher than 85% at all potentials.

In Figure 1b, it is shown how Pd and Al alternate their selectivity towards DHMF and other products depending on the applied potential. Although the onset potential of each metal seems very different in the voltammetry, both electrodes generate DHMF from the same potential of -0.57 V. These electrodes show selectivity towards DHMF formation until ca. -0.9 V, below which potential the formation of other products becomes dominant.

As shown in Figure 1c, Co, Au, and Cu preferentially reduce HMF through hydrogenolysis. Cu is the most active electrode material for HMF hydrogenolysis, even though it exhibits the lowest overall reduction current. Co and Au show similar activity and selectivity to DHMF and other hydrogenolysis products.

From the above results, we conclude that the hydrogenation of HMF is not strongly catalyst dependent since all catalysts show almost identical onset potentials (-0.5 ± 0.1 V). However, the catalysts differ in their reaction pathways towards DHMF or other products. Compared to the glucose hydrogenation activity on transition metals, the maximum concentration of sorbitol was achieved on Au and Cu (ca. 0.15 mM cm^{-2} with 0.1 M glucose),[28] showing that HMF hydrogenation to DHMF and other products is at least an order of magnitude more active than glucose hydrogenation to sorbitol.

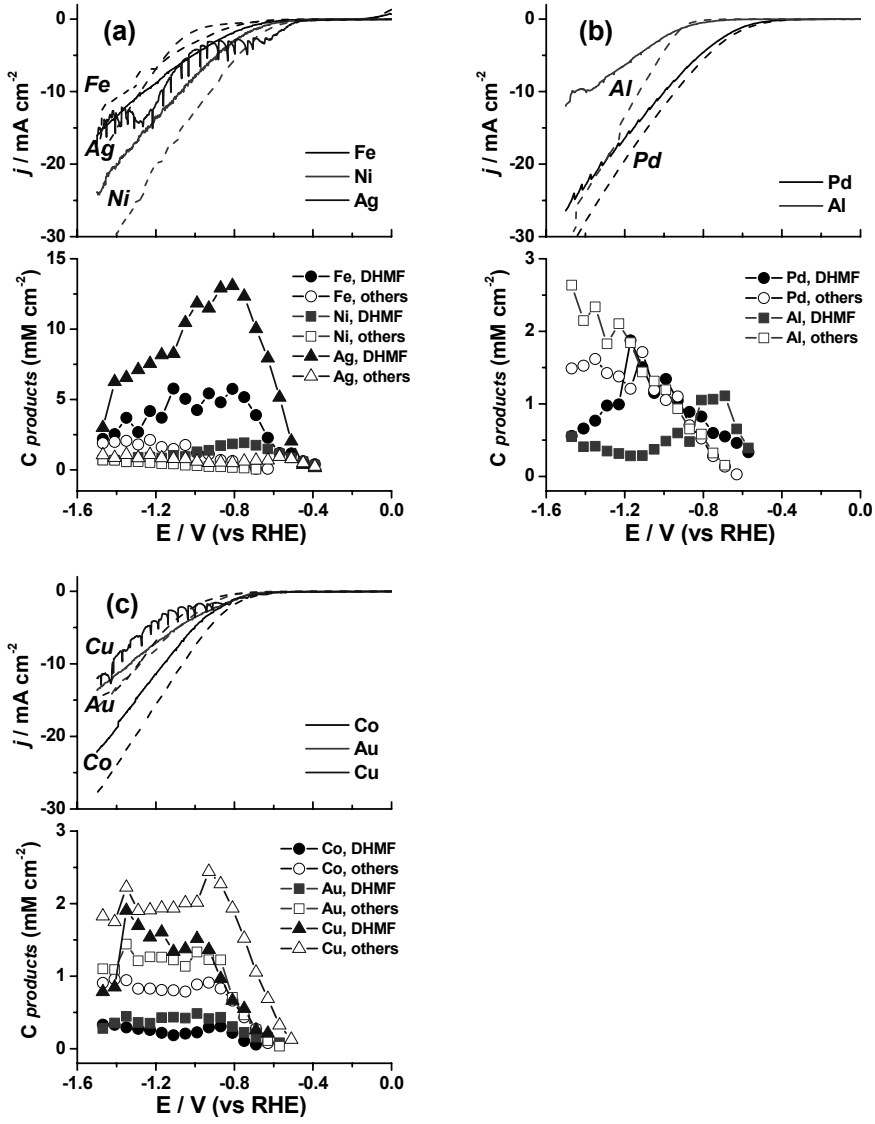

Figure 1. Electrocatalytic HMF (50 mM) reduction on Fe, Ni, and Ag, (b) Pd and Al, and (c) Co, Au, and Cu in 0.1 M Na_2SO_4. Current density profiles (upper panels) with (solid line) and without (dashed line) HMF in the solution during linear sweep voltammetry with a scan rate of 1 mV s^{-1}, and concentration profiles (lower panels) of corresponding reaction products, DHMF and others, as a function of potential.

The activity and selectivity of the post-transition *sp* metals (including Zn and Cd) are shown in Figure 2. An important difference between *sp* metals and *d* metals is the wider potential window on the *sp* metals due to their poor HER activity. Figure 2 shows the voltammograms of blank (dashed line) and of 50 mM HMF (solid line) reduction in 0.1 M Na_2SO_4 alongside the concentration profiles of the reaction products, DHMF and others, on (a) Zn, Cd, and In, (b) Bi and Pb, and (c) Sn and Sb. In general, the onset potential for hydrogen evolution in the blank scans is more negative than -1 V, which clearly differentiates the hydrogenation current of HMF from that of HER. In Figure 2a, the cathodic current with HMF on Zn, Cd and In increases from ca. -0.7 V, which is a ca. 300 mV less negative potential than that of blank. The current profile with HMF in solution is very similar to that of the Ag electrode in Figure 1a. Zn, Cd and In reduce HMF primarily to DHMF starting at ca. -0.65 V. Zn is the most active material until the production of DHMF decreases from -1.07 V, the potential at which the HER starts on Zn. Therefore we suspect that the HER interferes with the hydrogenation of 'C=O' of HMF. On Cd and In, the production of DHMF remain constant at negative potentials. On Cd, the selectivity towards DHMF appears to increases to 90% with the onset of the HER on Cd.

The voltammograms for HMF reduction on Bi and Pb in Figure 2b are similar to those in Figure 2a. DHMF and others are generated simultaneously from ca. -0.66 V. However, the selectivity towards DHMF on both electrodes is lower than those towards other hydration products before HER starts. In the potential region of the HER, the concentration of DHMF significantly increases from -1.29 V on Pb and -1.41 V on Bi, respectively. On the other hand, the formation of other products is suppressed during HER.

In Figure 2c, Sn shows a higher overpotential for HER in the blank voltammogram compared to that of Sb. However HMF reduction starts at the same potential. Both electrodes show a low activity to generate DHMF. The other products on Sn are first observed from -0.63 V, which is 120 mV earlier than that of DHMF. The concentration of DHMF is constant below -1 V and its selectivity is lower than 30%. The hydrogenolysis activity of Sn during HMF hydrogenation is consistent with the result of glucose reduction since Sn showed a 90% selectivity to 2-deoxysorbitol, also a hydrogenolysis product.[28] DHMF and other products on Sb are observed from -0.69 V. The initial selectivity of DHMF is 39%, however it gradually decreases and no DHMF is observed below -1.59 V.

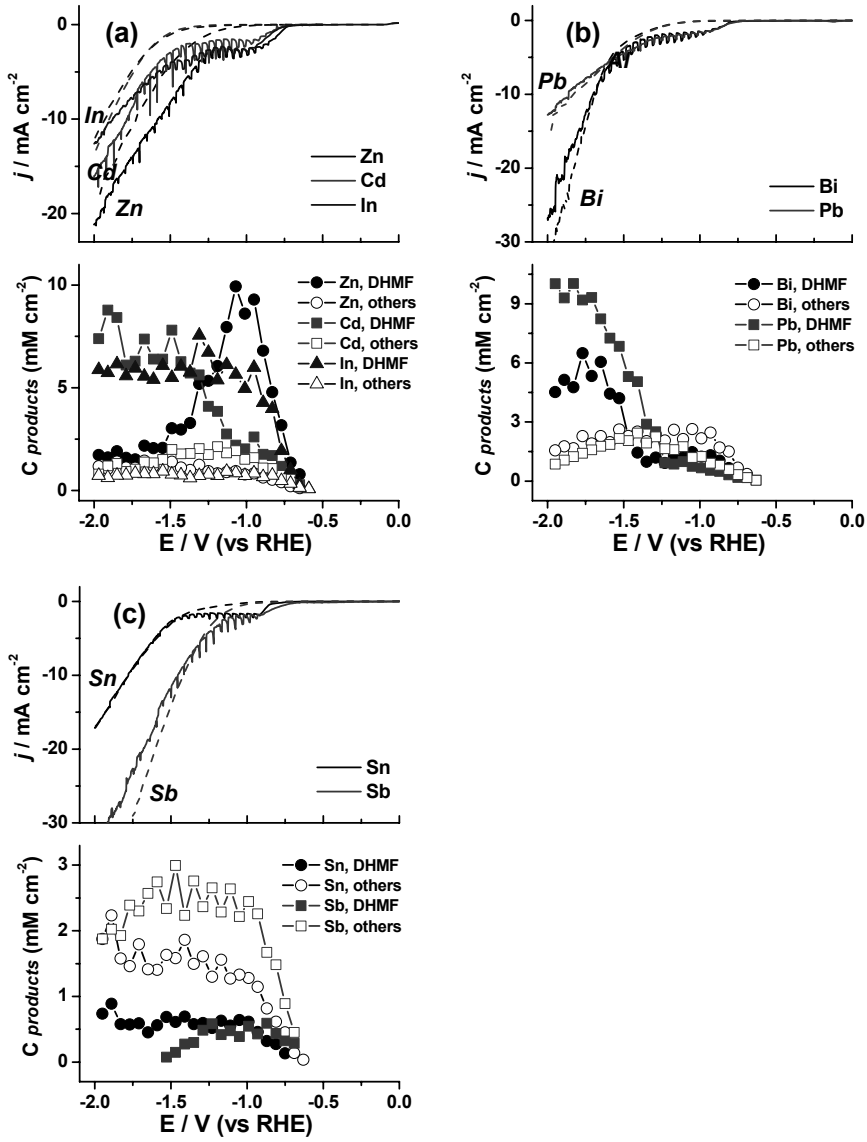

Figure 2. Electrocatalytic HMF (50 mM) reduction on Zn, Cd, and In, (b) Bi and Pb, and (c) Sn and Sb in 0.1 M Na_2SO_4. Current density profiles (upper panels) with (solid line) and without (dashed line) HMF in the solution during linear sweep voltammetry with a scan rate of 1 mV s^{-1}, and concentration profiles (lower panels) of corresponding reaction products, DHMF and others, as a function of potential.

For the poor metal electrodes, we can conclude that in agreement with the transition metals, HMF hydrogenation appears to be a non-catalytic reaction. However, there are still differences between catalysts in terms of their selectivity towards DHMF and other products. The HER on poor metals appears to influence the generation of DHMF; DHMF formation on Bi and Pb is enhanced by HER, however HER appears to suppress DHMF formation on Zn and Sb.

8.3.2 HMF reduction in the presence of glucose

Glucose and HMF are generated from acid-catalyzed cellulose hydrolysis,[29] however their reactivity during hydrogenation is quite different. From our previous work on glucose hydrogenation,[28] we demonstrated different affinities of various catalysts towards hydrogen formation (early transition and Pt group metals), sorbitol formation (late transition metals), and sorbitol and 2-deoxysorbitol formation (post-transition metals including Zn and Cd). However, from the trend of HMF hydrogenation described in the previous section, there is no clear correlation between the electronic structure of the catalysts and the product distribution. In addition, the onset potential for HMF hydrogenation seems to be more or less constant and not influenced by HER. It is of interest to study the hydrogenation of a mixture of HMF and glucose to gain insight into how they influence each other. Specifically, we selected a relatively low concentration of HMF (10 mM) compared to that of glucose (0.1 M) in order to mimic their ratio during acid-catalyzed cellulose hydrolysis. The concentration of HMF is lowered from 50 to 10 mM due to the unstability of sampling pump in a viscous solution.

3 shows the voltammograms of the blank (dashed line) and of 10 mM HMF + 0.1 M glucose (solid line) reduction in 0.1 M Na_2SO_4 alongside the concentration profiles of the reaction products on transition metals (a) Fe, Ni, and Ag, (b) Pd and Al, and (c) Co, Au, and Cu. We note that the presence of glucose in the solution does not change the general trend of current profiles compared to Figure 1, although a tenfold higher concentration of glucose (0.1 M) than that of HMF (10 mM) is added. Surprisingly, the glucose hydrogenation product, sorbitol, is not observed at any potential on any of the transition metals in Figure 3. However, the presence of glucose in solution changes the product distributions of HMF reduction. In Figure 1a, the onset potential of DHMF on Fe, Ni, and Ag is -0.39 V. However, with glucose in the solution it changes to -0.45 V on Fe, -0.21 V

on Ni, and -0.51 V on Ag, respectively. The delay of the onset potential on Fe and Ag may be explained by adsorbed glucose on the catalyst surface, but glucose accelerates HMF hydrogenation on Ni. The formation of other products generated through hydrogenolysis of HMF, is strongly suppressed at high potentials and only traces are observed on Fe and Ag. Interestingly, HER influences the product selectivity so that the concentration of DHMF decreases on Ni and Ag after hydrogen evolution starts. However, HMF reduction on Fe is less influenced by HER.

HMF reduction on Pd and Al is shown in Figure 3b. Hydrogenolysis products are dominant on these two metals, though glucose appears to enhance the DHMF production on Al. Also the onset potential for DHMF formation on Pd is 0.3 V less negative than that in Figure 1b. As a similar trend was observed on Ni in Figure 3a, we suspect that the presence of glucose enhances the hydrogenation activity on Ni and Pd, which both absorb hydrogen.[36]

Voltammograms of Co, Au, and Cu in Figure 3c are similar to those in Figure 1c, however the product distribution is different in the presence of glucose. First of all, DHMF formation on these three metals is observed from the onset potential and the formation of other products is delayed. Interestingly, the concentration of DHMF and others on Co in the presence of glucose is significantly higher than that in Figure 1c, although the concentration of HMF is 5 times lower. On Au and Cu, glucose also enhances the formation of DHMF with the suppression of other products. Suppression of DHMF formation on Cu is observed below -0.69 V when HER starts.

Similar to transition metals in Figure 3, poor metals also show different activity and selectivity in the presence of glucose. The main difference of the poor metals compared to the transition metals is that poor metals show activity towards glucose hydrogenation to generate sorbitol and 2-deoxysorbitol, also in the presence of HMF. Glucose enhances the formation DHMF on Zn, Cd, and In in Figure 4a, but the hydrogenolysis of HMF is blocked similarly to the transition metals.

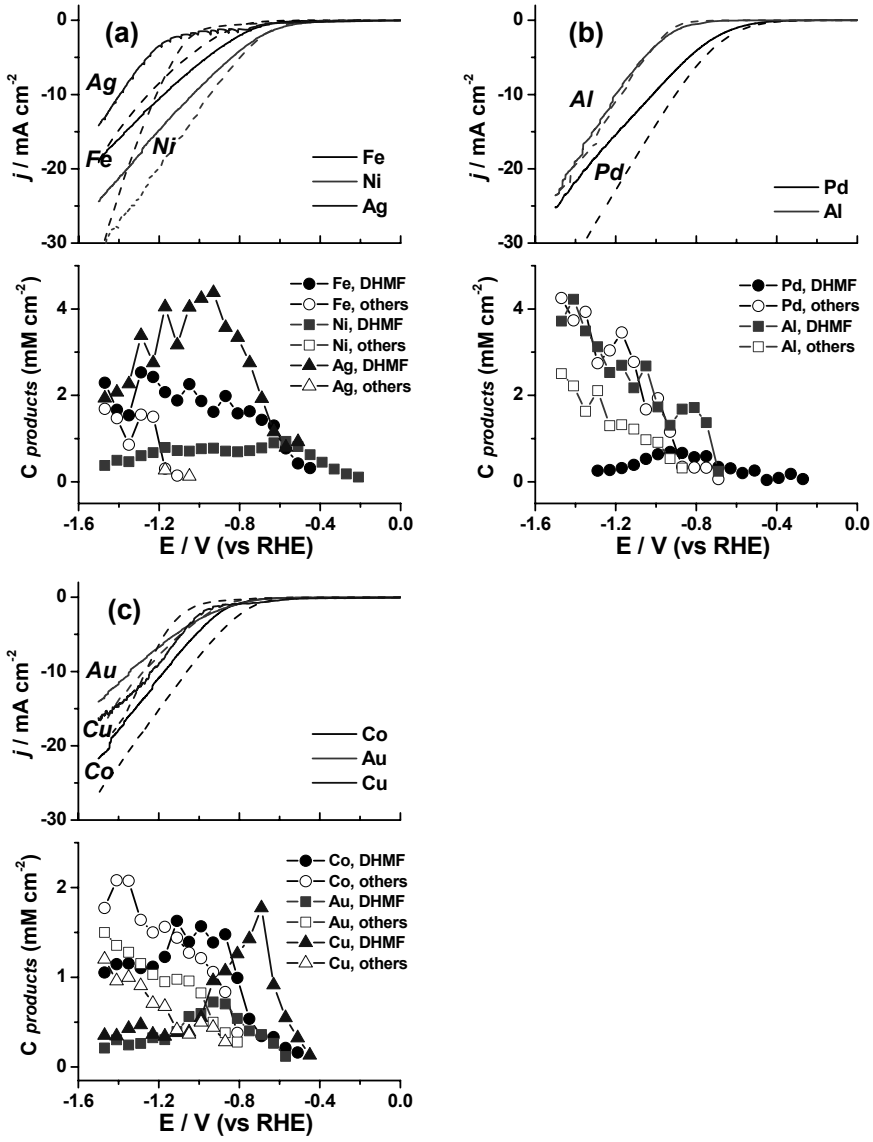

Figure 3. Electrocatalytic HMF (10 mM) + glucose (0.1 M) reduction on (a) Fe, Ni, and Ag, (b) Pd and Al, and (c) Co, Au, and Cu in 0.1 M Na_2SO_4. Current density profiles (upper panels) with (solid line) and without (dashed line) HMF + glucose in the solution during linear sweep voltammetry with a scan rate of 1 mV s^{-1}, and concentration profiles (lower panels) of corresponding reaction products, DHMF and others, as a function of potential.

The effect of glucose on HMF reduction on Pb, Sn, and Sb in Figure 4 is also rather small. Note that highest concentration of sorbitol (0.5 mM cm^{-2}) is observed on Pb, which is consistent with the activity of Pb for glucose hydrogenation to sorbitol.[28] On Sn, the selectivity of DHMF is within 15 - 40% in the whole potential range and glucose is not hydrogenated. The hydrogenolysis of HMF on Sb is accelerated in the presence of glucose especially from the potential where HER starts.

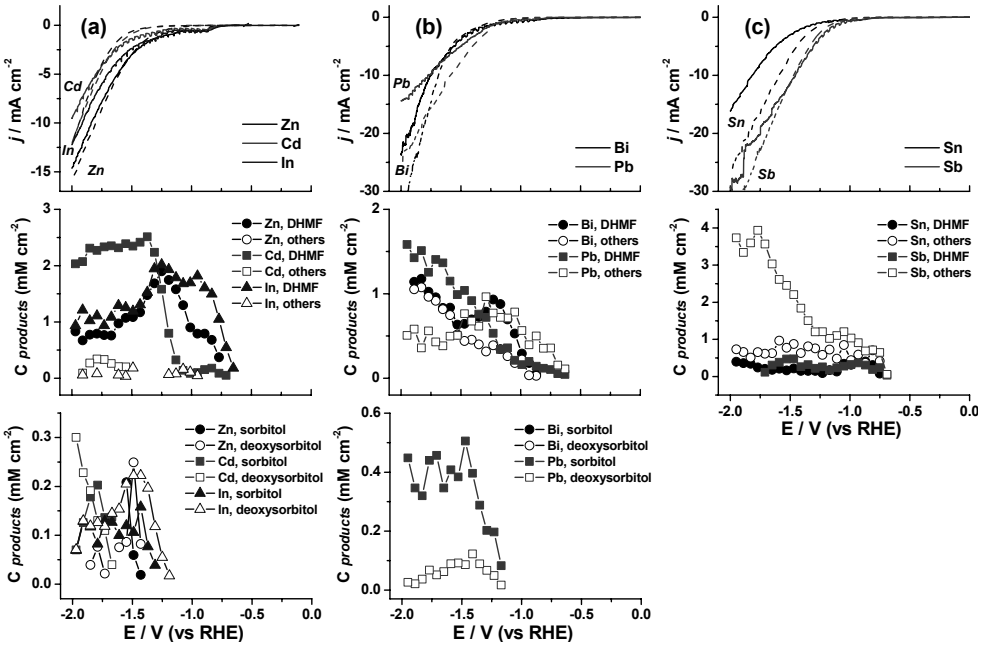

Figure 4. Electrocatalytic HMF (10 mM) + glucose (0.1 M) reduction on (a) Zn, Cd, and In, (b) Bi and Pb, and (c) Sn and Sb in 0.1 M Na_2SO_4. Current density profiles (upper panels) with (solid line) and without (dashed line) HMF + glucose in the solution during linear sweep voltammetry with a scan rate of 1 mV s^{-1}, and concentration profiles (middle and lower panels) of corresponding reaction products, DHMF and others (middle panel), sorbitol and 2-deoxysorbitol (lower panel), as a function of potential.

Based on our observations we conclude that on transition and poor metals, the presence of HMF blocks the reduction of glucose. On the other hand, glucose enhances the formation of DHMF and suppresses the hydrogenolysis of HMF on all transition metals and some (Zn,

Cd, and In) poor metals. However the influence of glucose on HMF reduction on Bi, Pb, Sn, and Sb is relatively limited.

8.3.3 A mechanistic view of HMF hydrogenation

From the relationship between voltammetry and reaction product distribution of HMF hydrogenation in the absence and the presence of glucose as shown in Figure 1-4, we conclude that the hydrogenation of HMF is always dominant and the reduction of glucose is strongly suppressed by the presence of HMF. Interestingly, the hydrogenation of HMF does not seem to be depend on the nature of the electrocatalyst, suggesting a non-catalytic reaction, based on the almost identical onset potentials (-0.5 ± 0.1 V) on all metals. This indicates that H_{ads} on metal surface is unlikely to be involved in the initial HMF hydrogenation process, which is different from general hydrogenation mechanisms of organic molecules.[37] Therefore, we assume that the initial HMF hydrogenation occurs directly by water molecules from the electrolyte:

$$HMF + 2\ H_2O + 2\ e^- \leftrightarrow DHMF + 2\ OH^- \quad (1)$$

A similar hydrogenation mechanism, not involving H_{ads}, has been suggested for the NO adsorbate reduction on Pt.[38]

As the onset potential of HMF hydrogenation is not strongly catalyst dependent, we can assume that other conductive materials can also be used as potential catalysts for HMF hydrogenation. To this end, we tested pyrolytic graphite (PG) and polycrystalline platinum for HMF reduction in 0.1 M Na_2SO_4 as shown in Figure 5. PG is normally used as a catalyst for oxygen reduction reaction (ORR) in alkaline[39] or as a stable catalyst support[40] in electrochemistry, however it does not show catalytic activity for glucose hydrogenation.[41] Polycrystalline Pt shows very limited activity towards the hydrogenation of glucose to sorbitol[28] due to its high affinity to generate hydrogen.[28] From the blank voltammograms, the HER starts from ca. -0.9 V on PG and ca. -0.3 V on Pt, respectively. The onset potential of HMF reduction on PG is ca. -0.65 V, which is a similar onset potential of HMF reduction on other metals. From ca. -0.7 V, we observe other hydrogenolysis products on PG. In contrast, DHMF is dominantly observed from ca. -0.4 V

on Pt. Therefore, these experiments confirm our hypothesis that the HMF reduction is a non-catalytic reaction.

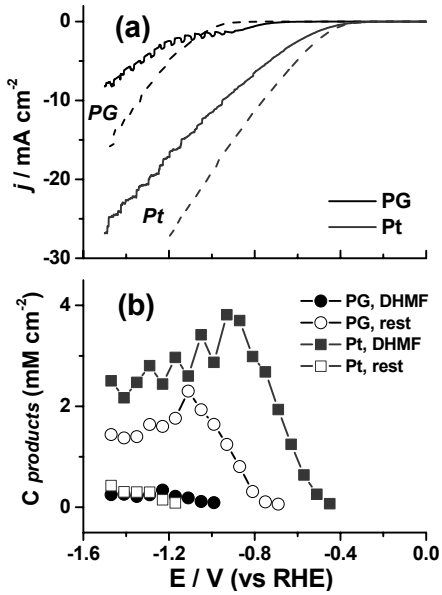

Figure 5. Electrocatalytic HMF (50 mM) reduction on pyrolytic graphite (PG) and polycrystalline Pt coil in 0.1 M Na_2SO_4. Current density profiles (a) with (solid line) and without (dashed line) HMF in the solution during linear sweep voltammetry with a scan rate of 1 mV s^{-1}, and concentration profiles (b) of corresponding reaction products, DHMF and others, as a function of potential.

The potential degradation of HMF at high pH was also investigated. 10 mM HMF was added to 0.1 M NaOH in the absence and presence of oxygen. After one hour, we could not observe any isomerization, aldol-condensation, or expected HMF oxidation products (i.e. FDA, FFCA, FDCA) under both conditions, although it is known that HMF is not stable at elevated temperature in alkaline condition.[4] As we have shown previously, high pH is essential for glucose hydrogenation since the high pH near the electrode surface mutarotates the cyclic (inactive) form of glucose to linear (electroactive) form, which is considered as a rate-determining step.[42-44] Based on this observation, we conclude that HMF is more stable than glucose at high pH at room temperature and high pH is not an essential factor for HMF hydrogenation.

In addition to the effect of pH, there is a thermodynamic reason why the hydrogenation of HMF is more favorable than that of glucose. The enthalpy change for the glucose hydrogenation to sorbitol is ca. -10 kcal mol^{-1}, as hydrogenation reactions are typically exothermic, however the hydrogenation of HMF to DHMF has an enthalpy change of ca. -20 kcal mol^{-1},[45] which may explain the preferential hydrogenation of HMF instead of glucose. Under electrochemical conditions, the identical onset potentials (-0.5 ± 0.2 V) for HMF hydrogenation should be related to the equilibrium potential of the reaction. However, the equilibrium potential of HMF hydrogenation to DHMF is ca. 0.1 V, calculated based on the Gibbs free energy changes in the gas phase at 298 K,[46] which implies that the identical onset potential for the reaction is mainly attributed to the activation energy (ca. 0.5 V), which is not or hardly influenced by catalyst. Although the hydrogenolysis of HMF is energetically neutral, it is obvious that proton and electron transfer reactions are involved in the hydrogenolysis process. Additionally, the hydrogenation of C=C bond in the furan ring of HMF is thermodynamically more favored compared to DHMF formation (i.e. ΔH = -35 kcal mol^{-1} during DHMF hydrogenation to DHMTHF[45]). Therefore, we could observe the formation of 2,5-dimethyl-2,3-dihydrofuran as one of other products during HMF electrocatalysis in Figure 6.

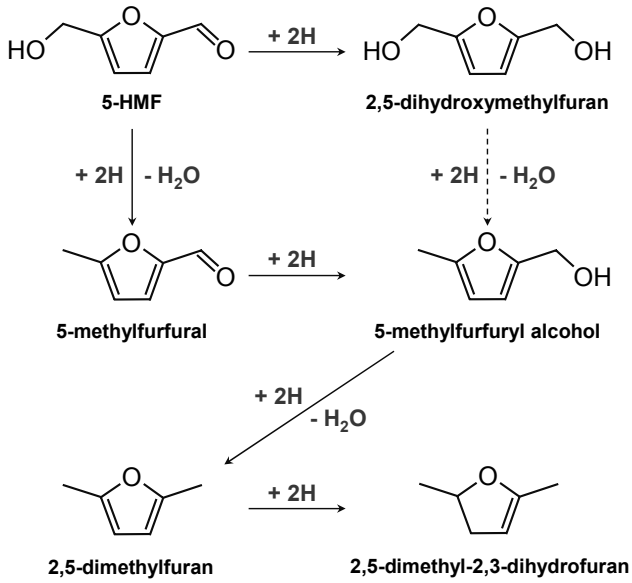

Figure 6. Schematic diagram of HMF hydrogenation pathways.

As shown in Scheme 1, the C=O group in HMF is hydrogenated to 2,5-dihydroxymethylfuran (DHMF) with 2H and 'others' are generated by hydrogenolysis of '-OH' in HMF during hydrogenation, leading first to 5-methylfurfural. To generate 2,5-dimethylfuran, the C=O moiety on 5-methylfurfural presumably first needs to be hydrogenated to 5-methylfurfuryl alcohol, although 5-methylfurfuryl alcohol is not observed from the product spectra. This indicates that the conversion rate of 5-methylfurfuryl alcohol to 2,5-dimethylfuran is extremely fast. Interestingly, DHMF is stable and not reduced to any significant extent on Ag, Cu, Pb, and Sn, highly active catalysts for HMF hydrogenation. Therefore, we conclude that 2,5-dimethylfuran derives from the hydrogenation of 5-methylfurfural through 5-methylfurfuryl alcohol, and not from DHMF. In a final step, one of the C=C bonds on 2,5-dimethylfuran is hydrogenated to 2,5-dimethyl-2,3-dihydrofuran, the most reduced reaction product observed in the GC-MS spectra. In addition to hydrogenated reaction products, we could also observe a certain amount of oxidized species (i.e. 2,5-furandicarbaldehyde) from HMF. We believe that the oxidation products are base-catalyzed reaction products, generated during electrolysis near the electrode surface. Although all the detailed concentrations of 5-methylfurfural, 2,5-dimethylfuran, and 2,5-dimethyl-2,3-dihydrofuran are not presented in Figures, the general reaction pathway shown in Figure 6 is consistent with the experimental data.

8.4 Conclusions

This chapter has studied the electrochemical 5-HMF hydrogenation in the absence and the presence of glucose on solid monometallic electrodes in neutral solution. We studied the activity and selectivity of the catalysts for HMF hydrogenation by correlating the voltammetric scan with online product analysis using HPLC, which provided qualitative and quantitative information regarding DHMF, other products from HMF hydrogenation, as well as sorbitol and 2-deoxysorbitol from the HMF and glucose mixture, as a function of potential. Three groups of catalysts regarding to reaction products from HMF hydrogenation were distinguished from this study. DHMF was mainly formed on Fe, Ni, Ag, Zn, Cd, and In. DHMF and other hydrogenolysis products were generated on Pd, Al, Bi, and Pb depending on the applied potential. Hydrogenolysis products of HMF are mainly formed on Co, Au, Cu, Sn, and Sb. The hydrogenation of HMF is not strongly catalyst dependent since all catalysts show a more or less identical onset potential (-0.5 ± 0.2 V),

mainly attributed to the activation energy which is not influenced by catalyst. However the intrinsic property of catalysts determines the reaction final product. Ag shows highest activity among all metals towards DHMF formation (with high selectivity > 85%). Some poor metals (Zn, Bi, Pb, and Sb) exhibit a change in selectivity for HMF reduction when hydrogen evolution takes place simultaneously. In the presence of glucose, the hydrogenation of HMF is always easier than glucose hydrogenation, on all metals. On transition metals, glucose enhances the formation of DHMF and suppresses the hydrogenolysis of HMF, whereas the glucose reduction itself is suppressed. On poor metals, glucose enhances the DHMF formation on Zn, Cd, and In. However, its influence on HMF reduction on Bi, Pb, Sn, and Sb is relatively limited. Since HMF can also be reduced on a graphite electrode, and the onset potential for HMF reduction is not very dependent on the nature of the electrode material, we conclude that the initial (reduction) step of HMF reduction is a non-catalytic reaction. In comparison to glucose, HMF hydrogenation does not require a high pH, such as generated close to the electrode surface during hydrogen evolution, a requirement necessary for glucose hydrogenation. As a result, the hydrogenation of glucose requires a higher overpotential than that of HMF. Finally, we note that this chapter's main aim was to scan the ability of various metals for electrochemical HMF hydrogenation by a combination of voltammetry and online HPLC. More quantitative information on efficiency and stability would require additional long-term electrolysis experiments. The current study may point towards the most interesting materials to choose for such a study.

8.5 References

[1] G. W. Huber, S. Iborra, A. Corma, *Chem. Rev*. **2006**, *106*, 4044-4098.

[2] A. Corma, S. Iborra, A. Velty, *Chem. Rev*. **2007**, *107*, 2411-2502.

[3] E.-S. Kang, D. W. Chae, B. Kim, Y. G. Kim, *J. Ind. Eng. Chem*. **2012**, *18*, 174-177.

[4] R.-J. van Putten, J. C. van der Waal, E. de Jong, C. B. Rasrendra, H. J. Heeres, J. G. de Vries, *Chem. Rev*. **2013**, *113*, 1499-1597.

[5] R. M. Musau, R. M. Munavu, *Biomass* **1987**, *13*, 67-74.

[6] C. Moreau, R. Durand, S. Razigade, J. Duhamet, P. Faugeras, P. Rivalier, P. Ros, G. Avignon, *Appl. Catal. A-Gen*. **1996**, *145*, 211-224.

[7] M. E. Zakrzewska, E. Bogel-Lukasik, R. Bogel-Lukasik, *Chem. Rev*. **2011**, *111*, 397-417.
[8] Z. Yuan, C. Xu, S. Cheng, M. Leitch, *Carbohydr. Res*. **2011**, *346*, 2019-2023.
[9] Q. Cao, X. Guo, J. Guan, X. Mu, D. Zhang, *Appl. Catal. A-Gen*. **2011**, *403*, 98-103.
[10] S. P. Simeonov, J. A. S. Coelho, C. A. M. Afonso, *ChemSusChem* **2012**, *5*, 1388-1391.
[11] F. S. Asghari, H. Yoshida, *Ind. Eng. Chem. Res*. **2006**, *45*, 2163-2173.
[12] D. Mercadier, L. Rigal, A. Gaset, J. P. Gorrichon, *J. Chem. Technol. Biotech*. **1981**, *31*, 489-496.
[13] K. Seri, Y. Inoue, H. Ishida, *B. Chem. Soc. Jpn*. **2001**, *74*, 1145-1150.
[14] H. Zhao, J. E. Holladay, H. Brown, Z. C. Zhang, *Science* **2007**, *316*, 1597-1600.
[15] A. A. Rosatella, S. P. Simeonov, R. F. M. Frade, C. A. M. Afonso, *Green Chem*. **2011**, *13*, 754-793.
[16] P. M. Grande, C. Bergs, P. D. de Maria, *ChemSusChem* **2012**, *5*, 1203-1206.
[17] S. P. Simeonov, J. A. S. Coelho, C. A. M. Afonso, *ChemSusChem* **2013**, *6*, 997-1000.
[18] C. Moreau, M. N. Belgacem, A. Gandini, *Top. Catal*. **2004**, *27*, 11-30.
[19] E. de Jong, M. A. Dam, L. Sipos, G.-J. M. Gruter, in *Biobased Monomers, Polymers, and Materials* (Ed.: P. B. Smith and R. A. Gross), *ACS Symposium Series*, **2012**, pp. 1-13.
[20] A. Gandini, *Green Chem*. **2011**, *13*, 1061-1083.
[21] K. R. Vuyyuru, P. Strasser, *Catal. Tod*. **2012**, *195*, 144-154.
[22] V. Schiavo, G. Descotes, J. Mentech, *B. Soc. Chim. Fr*. **1991**, 704-711.
[23] Y. Nakagawa, K. Tomishige, *Catal. Commun*. **2010**, *12*, 154-156.
[24] R. Alamillo, M. Tucker, M. Chia, Y. Pagan-Torres, J. Dumesic, *Green Chem*. **2012**, *14*, 1413-1419.
[25] T. Buntara, S. Noel, P. H. Phua, I. Melian-Cabrera, J. G. de Vries, H. J. Heeres, *Angew. Chem. Int. Ed*. **2011**, *50*, 7083-7087.
[26] Y. Roman-Leshkov, C. J. Barrett, Z. Y. Liu, J. A. Dumesic, *Nature* **2007**, *447*, 982-985.
[27] J. B. Binder, R. T. Raines, *J. Am. Chem. Soc*. **2009**, *131*, 1979-1985.
[28] Y. Kwon, M. T. M. Koper, *ChemSusChem* **2013**, *6*, 455-462.
[29] Y. Kwon, S. E. F. Kleijn, K. J. P. Schouten, M. T. M. Koper, *ChemSusChem* **2012**, *5*, 1935-1943.
[30] Y. Kwon, M. T. M. Koper, *Anal. Chem*. **2010**, *82*, 5420-5424.

[31] Y. Kwon, S. C. S. Lai, P. Rodriguez, M. T. M. Koper, *J. Am. Chem. Soc*. **2011**, *133*, 6914-6917.

[32] Y. Kwon, K. J. P. Schouten, M. T. M. Koper, *ChemCatChem* **2011**, *3*, 1176-1185.

[33] A. Santasalo-Aarnio, Y. Kwon, E. Ahlberg, K. Kontturi, T. Kallio, M. T. M. Koper, *Electrochem. Commun*. **2011**, *13*, 466-469.

[34] Y. Kwon, Y. Birdja, I. Spanos, P. Rodriguez, M. T. M. Koper, *ACS Catal*. **2012**, *2*, 759-764.

[35] P. Rodriguez, Y. Kwon, M. T. M. Koper, *Nat. Chem*. **2012**, *4*, 177-182.

[36] S. C. S. Lai, M. T. M. Koper, *Faraday Discuss*. **2008**, *140*, 399-416.

[37] J. M. Chapuzet, A. Lasia, J. Lessard, *Electrocatalysis*, ed. J. Lipowski, P. N. Ross, Wiley-VCH, New York, **1998**, 155– 196.

[38] A. C. A. de Vooys, G. L. Beltramo, B. van Riet, J. A. R. van Veen, M. T. M. Koper, *Electrochim. Acta* **2004**, *49*, 1307-1314.

[39] D. Qu, *Carbon* **2007**, *45*, 1296-1301.

[40] O. Brylev, M. Sarrazin, D. Belanger, L. Roue, *Appl. Catal. B-Env*. **2006**, *64*, 243-253.

[41] S. Fei, J. Chen, S. Yao, G. Deng, L. Nie, Y. Kuang, *J. Solid State Electrochem*. **2005**, *9*, 498-503.

[42] K. Park, P. N. Pintauro, M. M. Baizer, K. Nobe, *J. Electrochem. Soc*. **1985**, *132*, 1850-1855.

[43] A. Binkassim, C. L. Rice, A. T. Kuhn, *J. Appl. Electrochem*. **1981**, *11*, 261-267.

[44] P. N. Pintauro, D. K. Johnson, K. Park, M. M. Baizer, K. Nobe, *J. Appl. Electrochem*. **1984**, *14*, 209-220.

[45] H. Ed George W., Breaking the Chemical and Engineering Barriers to Lignocellulosic Biofuels: Next Generation Hydrocarbon Biorefineries, NSF, **2008**, 66-71.

[46] S. P. Verevkin, V. N. Emel'yanenko, E. N. Stepurko, R. V. Ralys, D. H. Zaitsau, A. Stark, *Ind. Eng. Chem. Res*. **2009**, *48*, 10087-10093.